



# Reach Your 100%

## Your success is our purpose

Your time is precious not only in terms of cost. However, a drug's journey from concept to patient takes years. You need to rely on products and services that ensure maximum efficiency at every step.

Our high-quality solutions are all engineered around the kind of functionality and intuitive performance necessary to speed up workflows, secure reproducibility, and accelerate the desired results.






Let's work together to make our world a better place.

[www.eppendorf.com/pharma](http://www.eppendorf.com/pharma)

## RESEARCH ARTICLE

WILEY

# Detection and phase I metabolism of the 7-azaindole-derived synthetic cannabinoid 5F-AB-P7AICA including a preliminary pharmacokinetic evaluation

Arianna Giorgetti<sup>1,2</sup>  | Lukas Mogler<sup>2,3</sup>  | Belal Haschimi<sup>2,3</sup>  | Sebastian Halter<sup>2,3</sup> | Florian Franz<sup>2,3</sup>  | Folker Westphal<sup>4</sup> | Svenja Fischmann<sup>4</sup> | Jan Riedel<sup>5</sup> | Michael Pütz<sup>5</sup> | Volker Auwärter<sup>2,3</sup> 

<sup>1</sup>Legal Medicine and Toxicology, University-Hospital of Padova, Italy

<sup>2</sup>Institute of Forensic Medicine, Forensic Toxicology, Medical Center - University of Freiburg, Germany

<sup>3</sup>Faculty of Medicine, University of Freiburg, Germany

<sup>4</sup>State Bureau of Criminal Investigation Schleswig-Holstein, Kiel, Germany

<sup>5</sup>Federal Criminal Police Office, Forensic Science Institute, Wiesbaden, Germany

## Correspondence

Volker Auwärter, Institute of Forensic Medicine, Forensic Toxicology, Medical Center - University of Freiburg, Germany.  
Email: volker.auwaerter@uniklinik-freiburg.de

## Funding information

European Union's Decentral Internal Security Fund (ISF), Grant/Award Number: IZ25-5793-2016-27 (ADEBAR); European Union's Justice Programme - Drugs Policy Initiatives, Grant/Award Number: 807055 - NPS-PRISON

## Abstract

In June 2018, a 'research chemical' labeled 'AB-FUB7AICA' was purchased online and analytically identified as 5F-AB-P7AICA, the 7-azaindole analog of 5F-AB-PINACA. Here we present data on structural characterization, suitable urinary consumption markers, and preliminary pharmacokinetic data. Structure characterization was performed by nuclear magnetic resonance spectroscopy, gas chromatography–mass spectrometry, infrared and Raman spectroscopy. Phase I metabolites were generated by applying a pooled human liver microsome assay (pHLM) to confirm the analysis results of authentic urine samples collected after oral self-administration of 2.5 mg 5F-AB-P7AICA. Analyses of pHLM and urine samples were performed by liquid chromatography–time-of-flight mass spectrometry and liquid chromatography–tandem mass spectrometry (LC–MS/MS). An LC–MS/MS method for the quantification of 5F-AB-P7AICA in serum was validated. Ten phase I metabolites were detected in human urine samples and confirmed *in vitro*. The main metabolites were formed by hydroxylation, amide hydrolysis, and hydrolytic defluorination, though – in contrast with most other synthetic cannabinoids – the parent compound showed the highest signals in most urine samples. The compound detection window was more than 45 hours in serum. The concentration–time profile was best explained by a two-phase pharmacokinetic model. 5F-AB-P7AICA was detected in urine samples until 65 hours post ingestion. Monitoring of metabolite M07, hydroxylated at the alkyl chain, next to parent 5F-AB-P7AICA, is recommended to confirm the uptake of 5F-AB-P7AICA in urinalysis. It seems plausible that the shift of the nitrogen atom from position 2 to 7 (e.g. 5F-AB-PINACA to 5F-AB-P7AICA) leads to a lower metabolic reactivity, which might be of general interest in medicinal chemistry.

## KEYWORDS

7-azaindole derivatives, human liver microsomes, mass spectrometry, new psychoactive substances

This is an open access article under the terms of the Creative Commons Attribution License, which permits use, distribution and reproduction in any medium, provided the original work is properly cited.

© 2019 The Authors. Drug Testing and Analysis published by John Wiley & Sons Ltd

## 1 | INTRODUCTION

Synthetic cannabinoids (SCs) are a class of exceptionally widespread recreational designer drugs and new psychoactive substances (NPS), produced to mimic the effects of *delta*-9-THC and sold as alleged legal and safe cannabis alternatives. Since the first identification of SCs in 'Spice' products, which dates back to 2008,<sup>1,2</sup> the European Monitoring Centre for Drugs and Drug Addiction (EMCDDA) has reported and identified more than 179 compounds pertaining to the subgroup of SCs, with a continuous production of novel molecules,<sup>3</sup> despite an overall decrease in the number of substances entering the market in the last years. Nevertheless, still more than 50 NPS per year were detected for the first time in Europe in 2017 and 2018.

Between 2013 and 2014, several indazole-based SCs, including *N*-(1-amino-3-methyl-1-oxobutan-2-yl)-1-(4-fluorobenzyl)-1*H*-indazole-3-carboxamide (semisystematic name: AB-FUBINACA), *N*-(1-amino-3-methyl-1-oxobutan-2-yl)-1-pentyl-1*H*-indazole-3-carboxamide (semisystematic name: AB-PINACA) and its 5-fluorinated analog *N*-[(1*S*)-1-(aminocarbonyl)-2-methylpropyl]-1-(5-fluoro)pentyl-1*H*-indazole-3-carboxamide (semisystematic name: 5F-AB-PINACA), were discovered on the Japanese drug market.<sup>4,5</sup> These compounds were shown to be full agonists at the CB<sub>1</sub> cannabinoid receptor with high potencies (CB<sub>1</sub> receptor binding and activation occur at low nanomolar concentrations).<sup>6-8</sup> *In vitro* studies have also shown that AB-PINACA displays a greater efficacy than *delta*-9-THC in activating the G-coupled proteins at CB<sub>1</sub> receptors and that some of its metabolites retain high affinity and activity.<sup>9</sup> Even if *in vivo* pharmacology and toxicology data related to these compounds are still lacking, some intoxications and even death cases have recently been reported in association to AB-FUBINACA, AB-PINACA, and 5F-AB-PINACA consumption.<sup>10-12</sup> A structurally related SC, methyl-[2-(1-(5-fluoropentyl)-1*H*-indazole-3-carboxamido)-3,3-dimethylbutanoate] (semisystematic name: 5F-MDMB-PINACA or 5F-ADB), which bears an aminoalkylindazole structure, was reported in associations with about 10 fatal intoxications in Japan and detected for the first time in a death case in 2014.<sup>13</sup> It was described as one of the most dangerous SCs<sup>11</sup> and detected in several autopsies after that.<sup>13-16</sup>

While the majority of SCs are characterized by an indole or indazole core structure, SCs with a 7-azaindole (7-AI) core structure have been synthesized and introduced into the NPS market most likely in response to regulations like the German act on the NPS (NpSG), and now represent about 3% of all monitored SCs<sup>3</sup>. Among these, a 7-AI analog of AB-FUBINACA, *N*-(1-amino-3-methyl-1-oxobutan-2-yl)-1-(4-fluorobenzyl)-1*H*-pyrrolo[2,3-*b*]pyridine-3-carboxamide (semisystematic name: AB-FUB7AICA; also referred to as AB-7-FUBAICA) entered the market as pure substance in powder form ('research chemical') and started to proliferate in online shops and NPS user forums. Recently, the 7-AI analog of 5F-ADB, methyl 2-(1-(5-fluoropentyl)-1*H*-pyrrolo[2,3-*b*]pyridine-3-carboxamido)-3,3-dimethylbutanoate (semisystematic name: 7'*N*-5F-ADB or 5F-MDMB-P7AICA) also appeared on NPS user forums. SCs of the 7-AI type usually present relatively low binding affinity and

functional activity at the CB<sub>1</sub> receptor.<sup>17,18</sup> From an analytical point of view, these compounds may lead to additional difficulties for identification, due to the similarity in physicochemical properties and identical masses with the corresponding indazole analogs. The occurrence of benzimidazole analogs or other azaindoles (carrying the nitrogen in 4, 5, or 6 position) could further complicate the situation, although such compounds have not been seized in large amounts so far, assuming that they have been correctly identified. In June 2018, a 'research chemical' labeled 'AB-FUB7AICA' was purchased online and analytically identified as a novel 7-AI-derived SC, *N*-(1-amino-3-methyl-1-oxobutan-2-yl)-1-(5-fluoropentyl)-1*H*-pyrrolo[2,3-*b*]pyridine-3-carboxamide (semisystematic name: 5F-AB-P7AICA) in our laboratory and reported to the EMCDDA. In Figure 1, chemical structures and semi-systematic names of these SCs are shown.

In both clinical and forensic settings, it is fundamental to prove an SC intake by the analysis of biological samples, with serum and urine samples being the most common matrices to screen for these compounds and their metabolites. In this context, the drug's post-dosing detectability as well as a clearance model are of major concern in forensic toxicology, as the detection windows for SCs are often short after acute intake and significantly longer after chronic use. Due to extensive metabolism, for most SCs the parent compound is rarely found in urine samples.<sup>19-22</sup> To the best of our knowledge, no pharmacokinetic data of this substance have been published.

The aim of the present study was to characterize and identify human phase I metabolites in human urine samples by means of liquid chromatography–time-of-flight mass spectrometry (LC–qToF–MS) and liquid chromatography–triple-quadrupole mass spectrometry (LC–MS/MS). As no commercially reference standards of 5F-AB-P7AICA phase I metabolites were available, reference spectra had to be generated *in vitro* using a pooled human liver microsome assay (pHLM). Finally, the most reliable urinary marker metabolites were evaluated, taking into consideration the pharmacokinetic profile of the substance.

## 2 | MATERIALS AND METHODS

### 2.1 | Chemicals and reagents

Methanol (HiPerSolv CHROMANORM<sup>®</sup>) for the solutions was purchased from VWR Chemicals (Darmstadt, Germany); ethyl acetate (p.a.) from Honeywell Riedel-de Häen<sup>®</sup> (Seelze, Germany); sodium carbonate (≥99.5%, anhydrous) and *n*-hexane (LiChrosolv) from Merck (Darmstadt, Germany); sodium hydrogen carbonate (≥99.5%, anhydrous), formic acid (Rotipuran<sup>®</sup> ≥98%, p.a.), and potassium hydrogen phosphate (≥99%, p.a.) from Carl Roth (Karlsruhe, Germany); acetonitrile (ACN) (LC–MS grade), ammonium formate 10 M (99.995%), potassium hydroxide (puriss. p. a. ≥ 86% (T) pellets), and superoxide dismutase (SOD) (≥3000 units/mg protein from bovine erythrocytes) from Sigma-Aldrich (Steinheim, Germany); pHLM (50 donors, 20 mg/mL



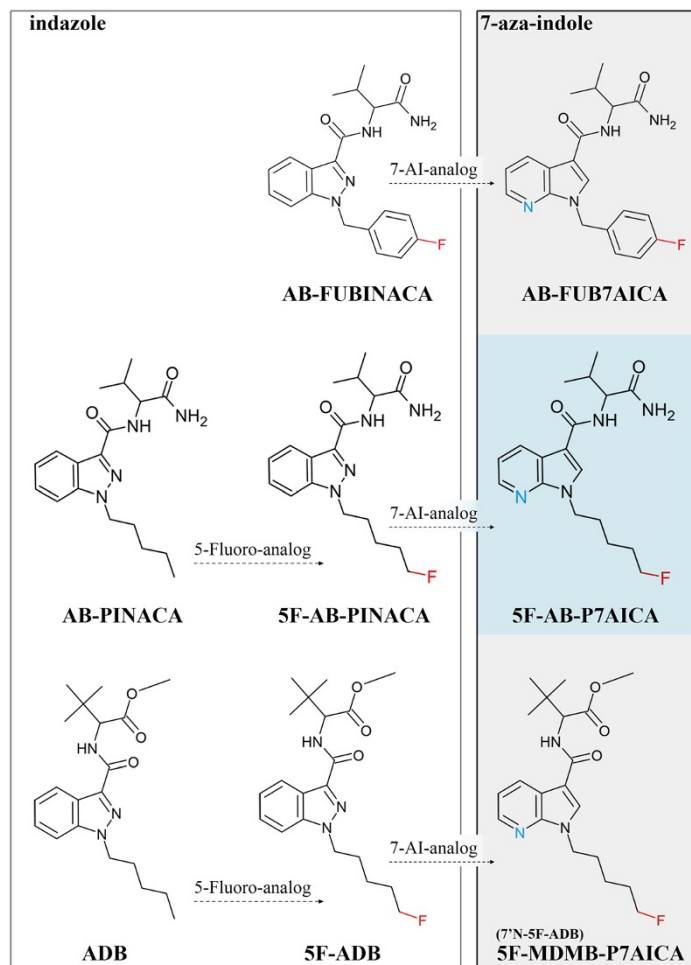


**FIGURE 1** Chemical structures and semisystematic names of synthetic cannabinoids mentioned [Colour figure can be viewed at [wileyonlinelibrary.com](http://wileyonlinelibrary.com)]

protein in 250 mM sucrose), NADPH regenerating solutions A and B (reductase activity 0.43  $\mu\text{mol}/\text{min}/\text{mL}$ ), and potassium phosphate buffer 0.5 M (pH 7.5) from Corning (Corning, NY, USA); and  $\beta$ -glucuronidase (*E. coli* K 12) from Roche Diagnostics (Mannheim, Germany).

Deionized water was prepared using a Medica<sup>®</sup> Pro deionizer from ELGA (Celle, Germany). Mobile phase A (1% v/v ACN, 0.1% v/v HCOOH, 2 mM ammonium formate in water) and mobile phase B (0.1% v/v HCOOH, 2 mM ammonium formate in ACN) were freshly prepared prior to analysis.

Deuterated methanol ( $\text{CD}_3\text{OD}$ ) was obtained from Euriso-top (Saarbrücken, Germany).

D5-JWH-200 (Internal standard or IS) was purchased from Chiron AS (Trondheim, Norway) and Cayman Chemical (Ann Arbor, MI, USA). A mix of SCs and one of SCs commercially available metabolites were also used. 5F-AB-P7AICA was purchased as a 'research chemical' named AB-FUB7AICA from an Internet shop. Identities and purities (>95%) of 5F-AB-P7AICA were confirmed by  $^1\text{H}$  nuclear magnetic resonance (NMR) spectroscopy and gas chromatography–mass spectrometry (GC–MS). Stock solutions (1 mg/mL) were prepared in ACN and stored at  $-20^\circ\text{C}$  until analysis.

## 2.2 | Structure elucidation

### 2.2.1 | Sample preparation (5F-AB-P7AICA)

5F-AB-P7AICA was analytically confirmed by GC–MS, NMR, infrared and Raman spectroscopy as described in the following sections. Furthermore, a solution of the compound was studied by liquid chromatography and electrospray ionization quadrupole time-of-flight mass spectrometry (LC–ESI–qToF–MS). Briefly, 1 mg 5F-AB-P7AICA was dissolved in 1 mL of methanol. Then, 10  $\mu\text{L}$  of this solution was evaporated to dryness at  $40^\circ\text{C}$  under nitrogen. Prior to the injection into the GC–MS system (injection volume: 1  $\mu\text{L}$ ), the sample was reconstituted in 100  $\mu\text{L}$  of dry ethyl acetate.

### 2.2.2 | GC–MS method

The GC–MS system consisted of a 6890 N-series gas chromatograph combined with a 5973-series mass selective detector and a 683 B series injector. The software used was Chemstation G1701GA version D.03.00.611. Mentioned products were purchased from Agilent (Waldbronn, Germany). The detailed method used is described elsewhere.<sup>23</sup>

Briefly, carrier gas was helium, injection port temperature was 270°C, flow rate 1 mL/min, oven temperature 100°C for 3 minutes, then ramped to 310°C at 30°C/min, 310°C were kept for 10 minutes. Electron ionization (EI, 70 V) was used and the MS was operated in scan mode ( $m/z$  40 to 550 amu). The obtained mass spectra were compared to commercially available EI-MS spectra libraries (Cayman Chemical, Wiley, MPW) and an in-house library of previously identified synthetic cannabinoids.

### 2.2.3 | Solid-state infrared spectroscopy (IR)

Nicolet 380 FT-IR spectrometer with Smart Golden Gate Diamond ATR. Software: OMNIC, Ver. 7.4.127 (Thermo Electron Corporation, Dreieich, Germany). Wavelength resolution: 4  $\text{cm}^{-1}$ ; scan range 650–4000  $\text{cm}^{-1}$ ; 32 scans/spectrum. IR spectra were recorded from salts and from free bases as neat film after following sample preparation procedure: For generation of the free bases, 2–5 mg of the salt were dissolved in demineralized water and were alkalized with one drop of NaOH (5% w/w). The solution was extracted with 1 mL diethylether, the ethereal phase was transferred in a new glass vial and the solvent was evaporated under a gentle nitrogen flow until the volume reached approximately 100  $\mu\text{L}$ . The remaining fluid was aspirated with a glass pipette and transferred directly on the ATR crystal where the remaining diethylether was continuously evaporated.

### 2.2.4 | Gas chromatography solid-state infrared spectroscopy

A GC-solid phase-IR (GC-sIR) system consisting of an Agilent GC 7890B (Waldbronn, Germany) with a probe sampler Agilent G4567A and a DiscovIR-GCTM (Spectra Analysis, Marlborough, MA, USA) was used. The column eluent was cryogenically accumulated on a spirally rotating ZnSe disk cooled by liquid nitrogen. IR spectra were recorded through the IR-transparent ZnSe disk using a nitrogen-cooled MCT detector.

GC parameters: injection: 1  $\mu\text{L}$  (approximately 2 mg compound in 2 mL appropriate solvent), splitless mode; injection port temperature: 240°C; carrier gas: helium; flow rate: 2.5 mL/min.

Chromatographic conditions: fused silica capillary DB-1column (30 m x 0.32 mm i.d., 0.25  $\mu\text{m}$  film thickness); oven temperature program: 80°C for 2 minutes, ramped to 290°C at 20°C/min, and held at for 20 minutes; transfer line: 280°C.

Infrared conditions: oven temperature: 280°C; restrictor temperature: 280°C; disc temperature: -40°C; dewar cap temperatures: 35°C; vacuum: 0.2 mTorr; disc speed: 3 mm/s; spiral separation: 1 mm; wavelength resolution: 4  $\text{cm}^{-1}$ ; IR range: 650–4000  $\text{cm}^{-1}$ ; acquisition time: 0.6 s/file; 64 scans/spectrum.

Data were processed using GRAMS/AI Ver. 9.1 (Grams Spectroscopy Software Suite, Thermo Fischer Scientific, Dreieich, Germany) followed by implementation of the OMNIC Software, Ver. 7.4.127 (Thermo Electron Corporation, Dreieich, Germany).

### 2.2.5 | Raman spectroscopy

B&W TEK Inc., i-Raman<sup>®</sup> Plus system: laser wavelength: 785 nm with BWS465-785S spectrometer: scan range: 174–3200  $\text{cm}^{-1}$ ; resolution: < 4.5  $\text{cm}^{-1}$  @ 912 nm and laser wavelength: 1064 nm with BWS485-1064S-05 spectrometer: scan range: 170–2502  $\text{cm}^{-1}$ ; resolution: ~ 9.5  $\text{cm}^{-1}$  @ 1296 nm, with BAC151B Raman Video Microsampling System: objective lens magnification: 20x; camera: active pixels: 1280 x 1024, Software: BWSpec<sup>®</sup> 4.03\_23\_C. Integration time (in ms) was chosen and adjusted in that way that a relative intensity preferably above 45 000 for the most intensive peak was reached. Additional information on parameters in spectrum title: sample\_mc (for microscope) \_wavelength\_laser power\_level\_integration time\_average number of recorded spectra. For the analysis of powders: the powder material was measured directly through a grip-bag or on a cap with the Video Microsampling System.

### 2.2.6 | NMR analysis

NMR spectra of the pure research chemical 5F-AB-P7AICA were recorded in DMSO- $d_6$  (1D and 2D spectra) at room temperature with a spectrometer Bruker AVANCE III HD 500 with probe: Bruker 5 mm CryoProbe Prodigy BBO with z-gradient. Sample preparation: approx. 10 mg of the sample were dissolved in deuterated solvents directly in the NMR tube. Measurement: All measurements were performed without sample spinning. Set of experiments used for structure elucidation: 1D-1H: 500 MHz, pulse program: zg, number of scans: 4.90° pulse, spectral width: 17 ppm, transmitter offset: 5.5 ppm, time domain: 128 k, spectrum size: 128 k, exponential multiplication with line broadening 0.2 Hz. 1D-13C: 125 MHz, pulse program: jmod (APT), number of scans: 512 or more. Assignments are supported by COSY, HSQC, and HMBC.

### 2.3 | In-vitro sample preparation (pHLM assay)

Microsomal incubations were performed as previously described.<sup>24,25</sup> Briefly, 5  $\mu\text{L}$  pHLM solution, 1  $\mu\text{L}$  parent compound stock solution (1 mg/mL 5F-AB-P7AICA in ACN), 5  $\mu\text{L}$  NADPH regenerating solution A, 1  $\mu\text{L}$  NADPH regenerating solution B, 10  $\mu\text{L}$  SOD, 20  $\mu\text{L}$  phosphate buffer and 58  $\mu\text{L}$  deionized water were incubated for 60 minutes at 37.5°C (100  $\mu\text{L}$  total assay volume). To quench the incubation, 100  $\mu\text{L}$  of ice-cold ACN were added. After centrifugation, the supernatant was transferred into a separate glass vial and stored at -20°C. Two negative control samples were prepared and processed accordingly: one solution containing no pHLM solution and one without the substrate (5F-AB-P7AICA). Prior to LC-MS/MS analysis, the supernatant was diluted 1:10 in mobile phase A/B (80:20, v/v). For LC-qToF-MS analysis, 100  $\mu\text{L}$  supernatant was evaporated until dryness and reconstituted in 25  $\mu\text{L}$  mobile phase A/B (80:20 v/v). Triplicates of pHLM incubates were performed and analyzed by LC-qToF-MS and LC-MS/MS. Applying the same conditions, a pHLM incubation with 1 mg/mL of 5F-AB-PINACA was also performed and results were compared to those obtained with 5F-AB-P7AICA.

## 2.4 | Self-administration study

A self-administration study, which does not require an approval by an ethics committee in Germany, was performed by one of the authors (Caucasian male, 32 years old, 80 kg body weight). The volunteer took a single oral dose of 2.5 mg of 5F-AB-P7AICA. Blank blood and urine samples were obtained from the subject directly before starting the experiment, which was performed at the Institute of Forensic Medicine in Freiburg (Germany) under medical supervision. Blood samples were collected from the cubital vein in S-Monovettes with clot activator, acquired from Sarstedt AG & Co (Nümbrecht, Germany) and immediately centrifuged. The serum obtained after centrifugation was transferred to separate glass vials and then stored at  $-20^{\circ}\text{C}$ . Sampling took place approximately every 10–20 minutes for the first 4 hours, then progressively lowering the frequency, till 3 days post administration. Blood samples were not collected during the night. Urine samples were collected during 3 days and also stored at  $-20^{\circ}\text{C}$  prior to analysis.

## 2.5 | In vivo sample preparation

### 2.5.1 | Serum sample preparation

The alkaline carbonate buffer (pH 10) was prepared by mixing 534 mL of a sodium carbonate solution (0.1 mol/L) and 466 mL of sodium hydrogen carbonate solution (0.1 mol/L). For preparation of Extraction Mixture 1, 990 mL of n-hexane and 10 mL of ethyl acetate (99:1, v/v) were mixed. For preparation of Extraction Mixture 2, 800 mL of n-hexane and 200 mL of ethyl acetate (80:20, v/v) were mixed. For analysis, a sample volume of 1 mL of serum and an alkaline liquid–liquid extraction was used. After the sample was fortified with 10  $\mu\text{L}$  of IS (*d5*-JWH-200, final concentration 1 ng/mL), 0.5 mL of carbonate buffer and 1.5 mL of Extraction Mixture 1 were added. Subsequent to gentle overhead mixing for 5 minutes, the sample was centrifuged at 4000 rpm for 20 minutes (Heraeus Megafuge 1.0, Thermo Scientific, Schwerte, Germany). Following this, 1 mL of the organic supernatant was transferred to a glass vial and evaporated to dryness under a gentle stream of nitrogen at  $40^{\circ}\text{C}$ . Extraction Mixture 2 (1.5 mL) was added to the remaining sample, which was processed accordingly (overhead mixing and centrifuging the sample, transferring the supernatant and evaporating to dryness with the same conditions). After complete evaporation, the sample was reconstituted in 100  $\mu\text{L}$  of mobile phase A/B (80:20, v/v).

### 2.5.2 | Urine sample preparation

A sample of 0.5 mL of urine was treated with 0.5 mL phosphate buffer (pH 6) and 30  $\mu\text{L}$   $\beta$ -glucuronidase for conjugate cleavage at  $45^{\circ}\text{C}$  for 60 minutes. Liquid–liquid extraction (LLE) was performed by adding 1.5 mL ACN and 0.5 mL of a 10 M ammonium formate solution. After overhead mixing for 5 minutes and centrifugation at 4000 rpm for 10 minutes (Heraeus Megafuge 1.0, Thermo Scientific, Schwerte, Germany) the organic layer was transferred into a separate glass vial and

evaporated to dryness under a nitrogen stream at  $40^{\circ}\text{C}$ . Reconstitution was done in 200  $\mu\text{L}$  mobile phase A/B (80:20, v/v) prior to LC–MS/MS analysis or in 25  $\mu\text{L}$  mobile phase A/B (80:20, v/v) prior to LC–qToF–MS analysis.

## 2.6 | LC–qToF–MS experiments

LC–qToF–MS analysis for metabolites was performed on an impact II™ qToF instrument coupled with an Elute HPLC system (both from Bruker Daltonik, Bremen, Germany). Chromatographic separation was achieved on a Kinetex® C18 column (2.6  $\mu\text{m}$ , 100  $\text{\AA}$ , 100  $\times$  2.1 mm; Phenomenex, Aschaffenburg, Germany), protected by an equivalent Security Guard™ ULTRA cartridge precolumn (Phenomenex, Aschaffenburg, Germany), applying gradient elution as follows: mobile phase B starting concentration was 20%, linearly increased to 25% in 2.5 minutes, further increased to 40% in 2.5 minutes, further increased to 65% in 1.5 minutes, further increased to 95% in 1.0 minutes, held for 1.0 minutes, decreased to starting conditions of 20% in 0.1 minutes and held for 1.4 minutes for re-equilibration. Total run time was 10 minutes. The total flow rate was set to 0.4 mL/min. The autosampler was cooled down to  $10^{\circ}\text{C}$ . Column oven temperature was  $40^{\circ}\text{C}$ . The injection volume was 10  $\mu\text{L}$ .

The qToF–MS was operated in positive ionization mode acquiring spectra in the range of  $m/z$  30–600 at an acquisition rate of 4.0 Hz. Full scan and broadband collision-induced dissociation (bbCID) data were acquired in one run. The collision energy applied for bbCID was  $30 \pm 6$  eV. Instrument parameters were set as described previously.<sup>24,25</sup> bbCID fragmentation experiments for 5F-AB-P7AICA were performed with the solution at 1  $\mu\text{g/mL}$ , with LC–qToF–MS parameters stated above. Results were compared with 1  $\mu\text{g/mL}$  of a reference standard solution of 5F-AB-PINACA, analyzed with the same method. HyStar™ version 3.2 and DataAnalysis version 4.2 (both from Bruker Daltonik, Bremen, Germany) were used for data acquisition and processing, respectively. pHLM incubations and authentic urine sample (sample #04) were also studied by LC–qToF–MS.

## 2.7 | LC–ESI–MS/MS experiments

LC–ESI–MS/MS analysis was performed with an Ultimate 3000RS UHPLC (Dionex, Sunnyvale, CA, USA) coupled to a QTRAP® 6500 triple quadrupole-linear ion trap instrument (SCIEX, Darmstadt, Germany). Chromatographic parameters, injection volume, autosampler and column oven temperature were as described above (paragraph 2.6).

The QTRAP–MS was operated with positive ionization in multiple reaction monitoring (MRM) mode and enhanced product ion (EPI) scan mode. The respective potentials [declustering potential (DP), entrance potential (EP), collision energy (CE), and collision cell exit potential (CXP)] of the precursor ion and main product ions were optimized under direct infusion of a 10 ng/mL solution (Table S1).

For metabolite identification EPI scan experiments with the hypothetical masses of anticipated phase-I metabolites were conducted and the obtained spectra were compared with the EPI spectrum of

the parent compound. All detected precursor ions were further characterized by EPI scans.

## 2.8 | In vitro and in vivo metabolite identification

Metabolites generated in the pHLM assay were tentatively identified and characterized by means of LC–qToF–MS. On the basis of previous studies regarding the metabolism of structurally related SCs, particularly of AB-PINACA and 5F-AB-PINACA,<sup>26,27</sup> a list of hypothetical metabolites, most probably formed in vitro and in vivo, was generated. Data were processed manually, applying the following criteria: MS peak area  $> 1 \times 10^5$  cps, mass error of the precursor ion  $< 5$  ppm, signal-to-noise ratio  $> 3:1$  and mass tolerance for fragment ions  $\pm 10$  ppm. To avoid missing the main metabolites, precursor ions were searched in the full scan data which were coeluting with typical fragment ions ( $m/z$  145 and  $m/z$  233<sup>22</sup>) in the bbCID data. Subsequently, EPI spectra of each metabolite precursor mass identified by LC–qToF–MS was recorded by LC–MS/MS. Therefore, EP was set to 10 V and a CE of 35 V with a spread of  $\pm 15$  V was applied. Once identified the most abundant fragment ions for each precursor mass, an LC–MS/MS scheduled MRM-method (sMRM) was developed, comprising the two most abundant ion transitions of each metabolite.

Optimized MRM parameters of the parent compound (Table S1) were adopted for the selected ion transitions of the identified metabolites, assuming similar fragmentation behavior (Table S2 shows the optimized MS parameters for metabolites).

For each metabolite, a ratio between the two most abundant ion transitions was calculated and used as an identification criterion in the authentic urine samples.

For each fragment ion of each metabolite, the absolute mean peak area across the pHLM triplicates was calculated as a rough estimate of their concentrations. Furthermore, considering the most abundant fragment ion for each metabolite, metabolites were ranked by dividing the mean peak area of detected metabolites by the mean peak area of the most abundant one (M07).

Metabolites identified in vitro were confirmed in vivo by the analysis of the urine samples of the voluntary, analyzed by means of LC–MS/MS and LC–qToF–MS analysis. For this purpose, sample #04, identified as the sample with the most abundant signals through a preliminary LC–MS/MS run with the developed sMRM method, was used. The following criteria were used for identification: signal-to-noise ratio  $> 3:1$ ; peak area  $> 1 \times 10^4$  cps; retention time (RT)  $\pm 0.1$  minutes from the expected RT; matching EPI spectra (when in vitro reference spectra where available); variability of the ion ratio  $< 20\%$ ; metabolites which were not detected in the pHLM assay were additionally confirmed by accurate mass (LC–qToF–MS analysis). Following the identification process, the parent compound and the main metabolites were confirmed by the same criteria in all urine samples and assessed by their peak area to construct a ranking and a concentration-time profile. Ranking was assessed in two different samples (sample #04 and #07, collected 4.67 hours and 10.83 hours after oral intake, respectively) to check for differences overall all the urine samples, related to the distance from consumption.

## 2.9 | Method validation

The LC–MS/MS method for quantification of 5F-AB-P7AICA in serum samples was validated in accordance with the literature recommendations.<sup>28</sup> Analytical parameters validated included selectivity, linearity, accuracy, precision, limit of detection (LOD), limit of quantification (LOQ), and matrix effects. To assess selectivity, six serum samples from five individual non-drug users, five of which without (blank samples) and one of which with the addition of IS (zero sample), were analyzed. Moreover, two serum blank samples spiked with a mix of SCs and of a mix of commercially available SC metabolites were analyzed to check for interferences (i.e. co-eluting matrix peaks that could give rise to false positive or false negative results).

Linearity was assessed using an 8 point calibration curve (0.1, 0.5, 1, 2.5, 7.5, 15, 22.5, and 30 ng/mL). Six calibration batches, all including a blank serum sample and a blank serum sample spiked with IS only (zero sample, final concentration of IS: 1 ng/mL), were analyzed on six different days. An eight-point calibration curve was plotted using the ratio of peak area of analytes/peak area of IS versus the analyte concentration. A Grubbs test, a Cochran test, and a Mandel-F-test, as well as the best-fitting calibration model, were performed using Valistat 2.0 software (Arvecon GmbH, Walldorf, Germany), in accordance with the guidelines of the German Society of Toxicological and Forensic Chemistry (GTFCh).<sup>29</sup>

For the assessment of accuracy and precision, quality control samples of pooled serum spiked at concentrations of 1 ng/mL (QC low) and 10 ng/mL (QC high), were analyzed in two replicates for each concentration per day (intra-day precision), and on six consecutive days (inter-day precision). Accuracy and precision were obtained by bias calculation and relative errors.

LOD and LOQ were determined by analyzing a six-point calibration curve spiked in zero serum (0.025, 0.035, 0.05, 0.07, 0.09, and 0.1 ng/mL).

Matrix effects were assessed at two different concentrations (1 ng/mL and 10 ng/mL) by comparison of neat solutions of the analyte in the mobile phase A/B (80:20, v/v), pre-extraction and post-extraction spiked samples according to the protocol suggested by Matuszewski et al.<sup>30</sup>

## 2.10 | Pharmacokinetic data

The validated LC–MS/MS method was used for the quantification of 5F-AB-P7AICA in serum samples and allowed to build a concentration-time profile in serum with the samples collected after a single controlled oral self-administration of 5F-AB-P7AICA. A 'qualitative' concentration-time profile was also built for the parent compound and the main metabolites in urine specimens sampled after the intake (concentrations are represented by the corresponding peak area and were normalized to the creatinine concentration). The analysis of the urine samples was repeated after six months of freezing at  $-20^\circ\text{C}$ , in order to assess the stability of the hypothetical urinary biomarkers.

Data were analyzed using GraphPad Prism (version 7.00 for Mac, GraphPad Software, La Jolla, CA, USA, www.graphpad.com). Distribution and elimination data were calculated on a semi-logarithmic scale,



starting from the maximum serum concentration measured and applying a non-linear regression with one phase-fit and two phase-fit decay model. The models were compared to choose the best fit-to-data with the Akaike's Informative Criteria (AICc).

### 3 | RESULTS AND DISCUSSION

#### 3.1 | Structure elucidation

A GC-MS analysis of the 'research chemical' originally sold as 'AB-FUB7AICA' was performed. GC-MS spectrum is shown in Figure S1 (retention time 12.21 minutes). By comparing the mass spectrum with the GC-MS libraries, no compound which matched the spectrum could be found. Within the Cayman Spectral Library, a match of 64% was found with 5-fluoro-7-QUPAIC (quinolin-8-yl 1-(5-fluoropentyl)-1*H*-pyrrolo[2,3-*b*]pyridine-3-carboxylate). The structure of the main component of the 'research chemical' was analyzed by means of 1D and 2D-NMR and revealed a 7-AI core structure. Although AB-FUB7AICA contains a 7-AI core, there was no indication of the presence of a 4-fluorobenzyl moiety bound to the nitrogen in position 1 of the core structure. Both GC-MS and 1D/2D-NMR data confirmed that the 'research chemical' purchased online instead contained a 5-fluoropentyl group bound to the indole nitrogen, and was finally identified as 5F-AB-P7AICA by the EU-funded project ADEBAR. The complete analytical data in converted exchangeable data formats and as a report are available online.<sup>31,32</sup> Regarding purity measurements, <sup>1</sup>H and <sup>13</sup>C spectra allowed to assess the absence of contaminations greater than 5% (in sum) and of any solvent signals. Furthermore, no signals for water were detectable with IR, resulting in an estimated purity greater than 95%. For simple identification IR- and GC-sIR spectra are presented in Figures S2-S16.

LC-qToF-MS was used to investigate the fragmentation pathway of 5F-AB-P7AICA and to compare it to the indole analog 5F-AB-PINACA. As shown in Figure 2, 5F-AB-P7AICA showed a RT of 4.7 minutes, while 5F-AB-PINACA eluted at 6.3 minutes when the substances were analyzed with the same method used for metabolism study. Despite the short run time, the isomers could be separated and most of the metabolites showed baseline separation.

Five characteristic fragment ions could be detected for 5F-AB-P7AICA ( $[M + H]^+ = 349.2034$ ,  $[M + Na]^+ = 371.1854$ ) (Figure 3). The most abundant fragment ion 'a' ( $C_{13}H_{14}FN_2O^+$ ,  $m/z$  233.1085, mass error - 0.5 ppm) is consistent with the fluoro-pentyl-7-AI acylium ion (formed by  $\alpha$ -cleavage). An additional fragmentation of this structure resulted in the 'b' fragment ion ( $C_8H_5N_2O^+$ ,  $m/z$  145.0396, mass error

0.0 ppm), which corresponds to the indazole acylium ion after the loss of the 5F-pentyl chain. Elimination of the terminal carboxamide group leads to the production of fragment 'c' ( $C_{17}H_{23}FN_3O^+$ ,  $m/z$  304.1820, mass error - 1.4 ppm), as previously described for 5F-AB-PINACA.<sup>16</sup> The localization of double bond is not clarified and would require further analysis. Further HF elimination leads to fragment 'd' ( $C_{17}H_{22}N_3O^+$ ,  $m/z$  284.1757, mass error 3.6 ppm). Finally, the cleavage between the carbon and the nitrogen atoms at the carboxamide unit generates fragment 'e' ( $C_{18}H_{23}FN_3O_2^+$ ,  $m/z$  332.1769, mass error - 0.4).

5F-AB-PINACA not only displayed a different retention time, but also non-identical fragmentation pattern (Figure 3). Indeed, despite several similarities, two additional fragment ions ( $C_9H_6FN_2O^+$ ,  $m/z$  177.046, mass error - 0.5 ppm, no structure known, and  $C_{13}H_{13}N_2O^+$ ,  $m/z$  213.1022, mass error 0.0) were observed, according to previously published data.<sup>33</sup> Both substances showed extensive formation of sodium adducts ( $C_{18}H_{25}FN_4NaO_2^+$ ,  $m/z$  371.1854, mass error 0.5 ppm for 5F-AB-P7AICA; mass error 0.3 ppm for 5F-AB-PINACA).

#### 3.2 | In vitro metabolism

In total, 14 metabolites were detected in the pHLM assay samples. The following metabolic reactions were observed: mono- and di-hydroxylation, hydrolytic defluorination, elimination of hydrofluoric acid, dehydrogenation and amide hydrolysis. The metabolites were ordered from lower to higher retention times (RTs) and numbered accordingly. As expected, none of the previous were found in the negative control samples.

A qualitative ranking of the metabolites produced by in vitro phase I metabolism was obtained. As shown in Table S3, the mono-hydroxylated metabolites, particularly M07, M09, and M04, presented the most intense peaks, while amide hydrolysis (M13) and a di-hydroxylated metabolites (M01) were the lowest in the in vitro metabolite ranking.

#### 3.3 | In vivo metabolism

The parent compound was detected in the urine samples after oral self-administration, as the most intense peak in the majority of the urine samples (Figure S17). This has never been described in the metabolism of SCs, since parent compounds are only seen in high concentrated urine and, normally, the peak intensity is far lower than that of metabolites. The fragment ions detected for the parent substance ( $C_{17}H_{23}FN_3O^+$ ,  $m/z$  304.1820, mass error 2.3 ppm;  $C_{13}H_{14}FN_2O^+$ ,  $m/z$  233.1085, mass error 0.2 ppm and  $C_8H_5N_2O^+$ ,  $m/z$  145.0396, mass error - 0.6 ppm) were consistent with the aforementioned fragmentation pattern.

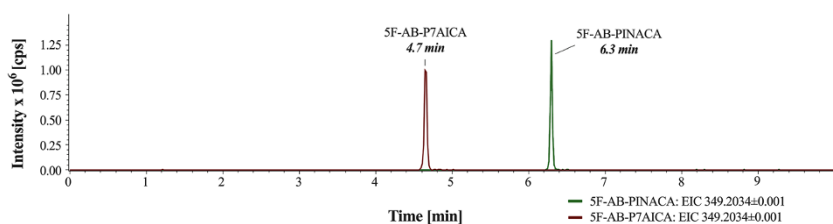


**FIGURE 2** Extracted ion chromatograms of 5F-AB-P7AICA and 5F-AB-PINACA after LC-qToF-MS analysis of 1  $\mu$ g/mL solutions in positive ionization full scan mode [Colour figure can be viewed at [wileyonlinelibrary.com](http://wileyonlinelibrary.com)]



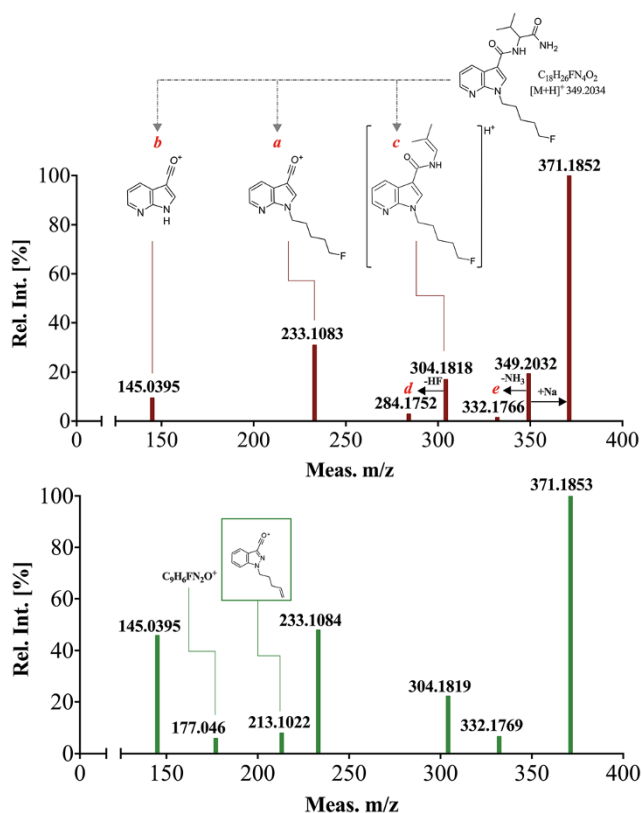


**FIGURE 3** LC-QToF-MS bbCID spectra showing the main characteristic fragment ions for 5F-AB-P7AICA (upper part) and 5F-AB-PINACA (lower part), with measured  $m/z$ . -HF: Elimination of hydrofluoric acid, -NH<sub>3</sub>: Loss of ammonia; +Na: Substitution of a proton with sodium [Colour figure can be viewed at [wileyonlinelibrary.com](http://wileyonlinelibrary.com)]

Overall, ten of the metabolites retrieved through pHLM analysis were confirmed in vivo in the urine sample of the volunteer (sample #04, which was characterized by the most intense signals in a preliminary LC-MS/MS analysis, was used for this purpose) (Figure S18). The in vivo metabolic reactions which generated the metabolites included hydroxylation, hydrolytic defluorination, dehydrogenation and amide hydrolysis. Parent compound or metabolites were not detected in any of the blank urine samples. Six of these in vivo phase I metabolites have been fully (including two fragment ions for each metabolite) confirmed in vitro by means of LC-qToF-MS/MS. For the other four metabolites, signal intensity was not sufficient to produce bbCID spectra and the confirmation required EPI spectra. The postulated metabolic pathway of 5F-AB-P7AICA is shown in Figure 4.

Due to the presence of isomeric compounds with identical fragment ions the unambiguous identification of the position of the functional groups introduced by metabolic reactions would require isolation of metabolites for structure elucidation, for example, by NMR spectroscopy or synthesis of reference material. Thus, the exact chemical structures of some metabolites remain unclear. In Table 1, the in vivo phase I metabolites are shown, in conjunction with the proposed biotransformation step, the tentative localization of the metabolic modification(s), the detected  $[M + H]^+$  precursor ion, the proposed elemental composition including the mass error,

characteristic fragment ions with proposed elemental composition and their mass errors and the rank position in two different authentic urine sample (samples #04 and #07). In Figure S19, EPI spectra of each metabolite, detected in vivo and in vitro, are provided.

M04, M06, M07, and M09, with  $[M + H]^+$  at  $m/z$  365.1983 suggest the molecular formula  $C_{18}H_{26}FN_4O_3^+$  and mass error - 3.4 ppm, 0.2 ppm, 0.3 ppm and - 1.9 ppm were consequently formed by an in vivo metabolic phase I reaction consistent with monohydroxylation. In the case of M04 and M07 the typical fragment ions include  $m/z$  249.1034 (mass error 1.7 ppm and - 2.8 ppm, respectively) and the unaltered indazole acylium ion. The latter allows to exclude that the hydroxylation took place at the core ring system. As the MS/MS spectra contained similar product ions, monohydroxylation at the 5-fluoropentyl side chain seem likely.

On the contrary, M06 and M09 produce the fragment ions at  $m/z$  233.1085 (mass error 1.3 ppm and - 0.5 ppm, respectively), suggesting a location of the mono-hydroxylation at the valine amide substituent, and at  $m/z$  145.0396 (mass error - 2.4 ppm and 1.3 ppm).

Further hydroxylation of M04 and M07 at the valine amide substituent or, as also possible, of M06 and M09 at the 5-fluoropentyl chain, led to the production of M01 and M03 ( $C_{18}H_{26}FN_4O_4^+$ ,  $m/z$  381.1932). These metabolites were formed by dihydroxylation and were characterized by both the unaltered acylium ion and hydroxylated fluoropentyl chain fragment ions, which were confirmed by means of EPI scan. Due to the relatively low signal intensities of these metabolites in the pHLM assay (cfr. rank #13 and #8, respectively; Table S3) it was not possible to confirm the molecular ions by means of LC-qToF-MS.

The exchange of the fluorine atom by a hydroxyl function occurred for M05 ( $C_{18}H_{27}N_4O_3^+$ ,  $m/z$  347.2078, mass error - 3.0 ppm), which is produced by human phase I metabolism through hydrolytic defluorination. Typical fragment ions, confirmed by LC-qToF-MS, were detected at  $m/z$  231.1128 (mass error 2.4 ppm) and at  $m/z$  145.0396 (mass error 2.0 ppm).

The same phenomenon occurred for M02, which is most probably formed by monohydroxylation in combination with hydrolytic defluorination. Fragment ions detected in the EPI scans (both in pHLM and in urine samples) were consistent with an exchange of the fluorine atom by a hydroxyl group and an additional hydroxylation at the pentyl chain ( $m/z$  247). The fragment ion of the 7-AI core ( $m/z$  145) remained unaltered.

As can be deduced from the accurate mass, M11 ( $C_{18}H_{24}FN_4O_2$ ,  $m/z$  347.1878, mass error - 2.4 ppm) is produced by the metabolic reaction of dehydrogenation. The detected fragment ions at  $m/z$  233.1085 (mass error - 1.2 ppm) and  $m/z$  145.0402 (mass error 2.0 ppm), suggest that the dehydrogenation does not involve the side chain, but most probably occurs at the valine amide scaffold.

Finally, M13 is most probably formed in vivo by amide hydrolysis. This metabolite was also found in the pHLM assay, though in extremely low signal intensities, and was confirmed by LC-qToF-MS analysis ( $C_{18}H_{25}FN_3O_3^+$ ,  $m/z$  350.1874, mass error - 3.5 ppm). Main fragments were detected at  $m/z$  233.1077 ( $C_{13}H_{14}FN_2O^+$ , mass error 4.5 ppm) and at  $m/z$  304.1820 ( $C_{17}H_{23}FN_3O^+$ , mass

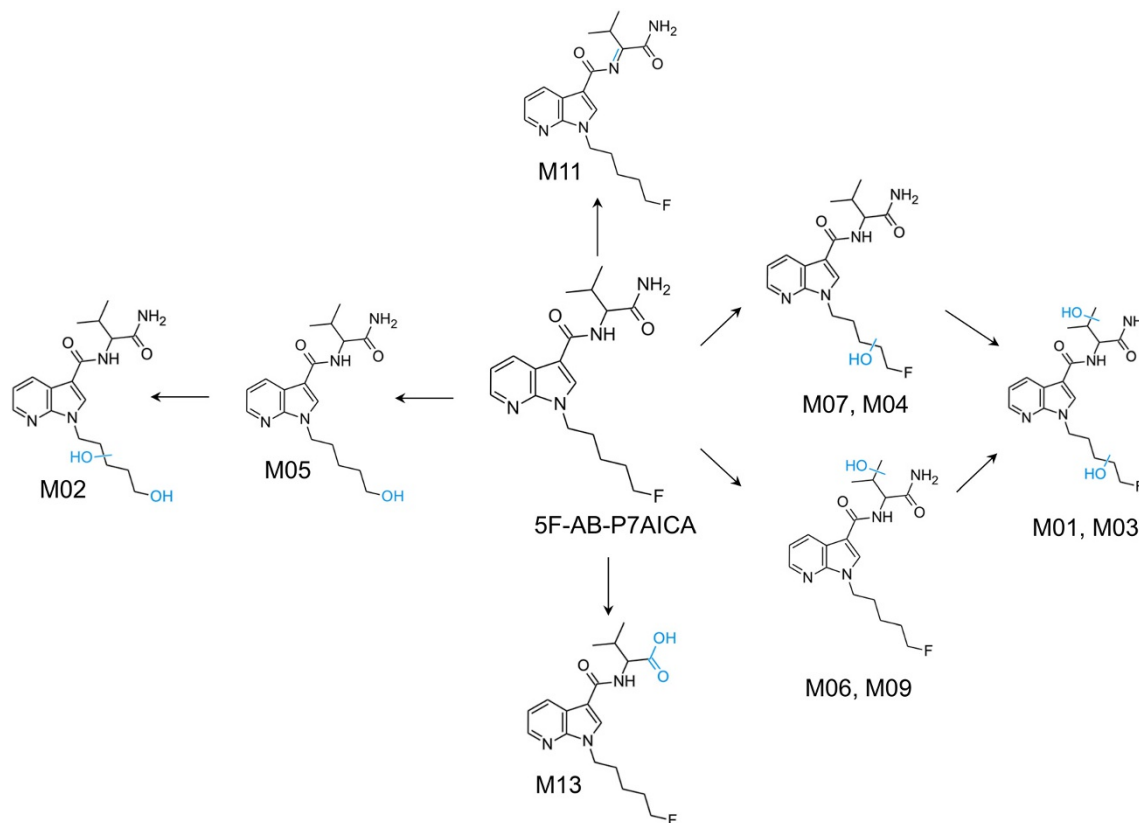


**FIGURE 4** Proposed human phase I biotransformation pattern of 5F-AB-P7AICA. The (tentative) localization of the metabolic reactions is highlighted in blue [Colour figure can be viewed at [wileyonlinelibrary.com](https://onlinelibrary.wiley.com/doi/10.1002/dm.2692)]

error – 0.3 ppm). In the urine sample, M13 could be confirmed by LC–qToF–MS analysis by the detection of  $[M + H]^+$  at  $m/z$  350.1874 (mass error 0.70 ppm), and its fragment ions at  $m/z$  304.1820 ( $C_{17}H_{23}FN_3O$ , mass error 2.60: ppm),  $m/z$  233.1085 ( $C_{13}H_{14}FN_2O$ , mass error – 2.10 ppm) and  $m/z$  145.0396 ( $C_8H_5N_2O$ , mass error -2.80 ppm).

Urine analysis did not show additional metabolites in the bbCID scan approach when compared to pHLM, indicating the usefulness of this type of in vitro assay in the process of identification of possible urinary biomarkers. It is known that pHLM could not perfectly reproduce the full spectrum of in vivo metabolism, as they are restricted to certain types of enzymes, mainly involve metabolic phase I reactions, and usually produce less metabolites formed by two or more metabolic reactions.<sup>21</sup> Moreover, the interpretation of comparisons of peak areas should be performed cautiously, as signal intensities are affected by matrix effects and might not only correlate with concentrations but display differing ionization efficiencies for different structures. Notwithstanding this limitation, the comparison offers the possibility of interpreting metabolite prevalence and tentatively identifying suitable urinary markers.

As for the identification of the preferred urinary biomarkers, in authentic urinary samples collected after an oral administration of 5F-AB-P7AICA, the parent compound showed the most intense peaks, until 28.83 hours after the intake. The most abundant metabolites in the urine samples changed during the concentration-time profile

analysis. Taking as a reference the sample with the most abundant peaks (sample #04, 4.67 hours after oral intake), parent compound excluded, the most abundant metabolites were the hydroxylation and hydrolytic defluorination products (M07, followed by M05 and M04). At the fourth rank position in the urine sample #04 (parent compound excluded) M13, the amide hydrolysis product, was seen. However, this ranking was not fixed overall all the urine samples. When considering another sample, e.g. sample #07 (10.83 hours after oral intake), M07 was followed by M13, while M05 was only located at the third place. After 29 hours (sample #15), the peak area of M13 exceeded the peak area of the parent compound. The re-analysis of the urine samples after 6 months of sample storage at  $-20^\circ\text{C}$  did not show changes in the relative abundances of parent compound and metabolites, thus confirming analyte stability under these storing conditions.

Although the unchanged parent compound has also been seen in human urine samples after AB-PINACA<sup>27</sup> and 5F-AB-PINACA consumption (own unpublished data), main metabolites were always much more abundant than the parent compound. For most of the SCs, the detection of parent compound is only seen in samples with extraordinarily high metabolite concentrations.<sup>19–22</sup> This discrepancy in the metabolic pattern between 5F-AB-P7AICA and 5F-AB-PINACA was confirmed by a comparison of the ratios between metabolites and parent compounds in pHLM assays: when comparing separate pHLM incubations of parent compounds after 1 hour of

**TABLE 1** High-resolution mass spectrometric data showing parent compound and metabolites from authentic urine sample in order of their retention times (RTs)

RT ID	RT [min]	Metabolic Reaction	Location of Metabolic Reaction	Ranking Position (sample #04, #07)	Ion ratio	Calculated [M + H] <sup>+</sup>	Ion Formula	Mass Error [ppm]	Diagnostic Production Calculated [m/z]	Diagnostic Product ion Formula	Diagnostic Product Ion Mass Error [ppm]
M01	1.2	Dihydroxylation	5FP + VA	#09; #09	50%	381.1933	C <sub>18</sub> H <sub>26</sub> FN <sub>4</sub> O <sub>4</sub> <sup>+</sup>	n.d.	249 145	C <sub>13</sub> H <sub>14</sub> FN <sub>2</sub> O <sub>2</sub> <sup>+</sup> C <sub>8</sub> H <sub>5</sub> N <sub>2</sub> O <sup>+</sup>	n.d. n.d.
M02	1.2	Defluorination + OH	5FP	#08; #08	22%	363.2026	C <sub>18</sub> H <sub>27</sub> N <sub>4</sub> O <sub>4</sub> <sup>+</sup>	-4.7	247 145	C <sub>13</sub> H <sub>17</sub> N <sub>3</sub> O <sub>2</sub> <sup>+</sup> C <sub>5</sub> H <sub>11</sub> NO <sub>2</sub> <sup>+</sup>	n.d. n.d.
M03	1.4	Dihydroxylation	5FP + VA	#07; #07	17%	381.1933	C <sub>18</sub> H <sub>26</sub> FN <sub>4</sub> O <sub>4</sub> <sup>+</sup>	n.d.	249 145	C <sub>13</sub> H <sub>14</sub> FN <sub>2</sub> O <sub>2</sub> <sup>+</sup> C <sub>8</sub> H <sub>5</sub> N <sub>2</sub> O <sup>+</sup>	n.d. n.d.
M04	2.0	Hydroxylation	5FP	#03; #04	20%	365.1983	C <sub>18</sub> H <sub>26</sub> FN <sub>4</sub> O <sub>3</sub> <sup>+</sup>	-3.4	249.1034 145	C <sub>13</sub> H <sub>14</sub> FN <sub>2</sub> O <sub>2</sub> <sup>+</sup> C <sub>8</sub> H <sub>5</sub> N <sub>2</sub> O <sup>+</sup>	1.7 n.d.
M05	2.1	Hydrolytic defluorination	5FP	#02; #03	28%	347.2078	C <sub>18</sub> H <sub>27</sub> N <sub>4</sub> O <sub>3</sub> <sup>+</sup>	-3.0	231.1128 145.0396	C <sub>13</sub> H <sub>15</sub> N <sub>2</sub> O <sub>2</sub> <sup>+</sup> C <sub>8</sub> H <sub>5</sub> N <sub>2</sub> O <sup>+</sup>	2.4 2.0
M06	2.1	Hydroxylation	VA	#06; #06	91%	365.1983	C <sub>18</sub> H <sub>26</sub> FN <sub>4</sub> O <sub>3</sub> <sup>+</sup>	0.2	233.1085 145.0396	C <sub>13</sub> H <sub>14</sub> FN <sub>2</sub> O <sup>+</sup> C <sub>8</sub> H <sub>5</sub> N <sub>2</sub> O <sup>+</sup>	1.3 -2.4
M07	2.3	Hydroxylation	5FP	#01; #01	12%	365.1983	C <sub>18</sub> H <sub>26</sub> FN <sub>4</sub> O <sub>3</sub> <sup>+</sup>	0.3	249.1034 145.0396	C <sub>13</sub> H <sub>14</sub> FN <sub>2</sub> O <sub>2</sub> <sup>+</sup> C <sub>8</sub> H <sub>5</sub> N <sub>2</sub> O <sup>+</sup>	-2.8 1.8
M09	3.0	Hydroxylation	VA	#05; #05	54%	365.1983	C <sub>18</sub> H <sub>26</sub> FN <sub>4</sub> O <sub>3</sub> <sup>+</sup>	-1.9	233.1085 145.0396	C <sub>13</sub> H <sub>14</sub> FN <sub>2</sub> O <sup>+</sup> C <sub>8</sub> H <sub>5</sub> N <sub>2</sub> O <sup>+</sup>	0.5 1.3
M11	4.3	Dehydrogenation	VA	#10; #10	61%	347.1878	C <sub>18</sub> H <sub>24</sub> FN <sub>4</sub> O <sub>2</sub> <sup>+</sup>	-2.4	233.1085 145.0396	C <sub>13</sub> H <sub>14</sub> FN <sub>2</sub> O <sup>+</sup> C <sub>8</sub> H <sub>5</sub> N <sub>2</sub> O <sup>+</sup>	-1.2 2.0
M00	4.6	5F-AB-P7AICA		#00; #00	51%	349.2034	C <sub>18</sub> H <sub>26</sub> FN <sub>4</sub> O <sub>2</sub> <sup>+</sup>	-1.2	233.1085 145.0396	C <sub>13</sub> H <sub>14</sub> FN <sub>2</sub> O <sup>+</sup> C <sub>8</sub> H <sub>5</sub> N <sub>2</sub> O <sup>+</sup>	1.4 -1.3
M13	5.4	Amide hydrolysis	VA	#04; #02	49%	350.1874	C <sub>18</sub> H <sub>25</sub> FN <sub>3</sub> O <sub>3</sub> <sup>+</sup>	-3.5	233.1085 145.0396 304.1820	C <sub>13</sub> H <sub>14</sub> FN <sub>2</sub> O <sup>+</sup> C <sub>8</sub> H <sub>5</sub> N <sub>2</sub> O <sup>+</sup> C <sub>17</sub> H <sub>23</sub> FN <sub>3</sub> O <sup>+</sup>	4.5 -2.8* -0.3

Rank position is shown in two different samples, collected 4.67 hours and 10.83 hours after oral intake (sample #04 and #07, respectively). M08, M10, and M12 are not shown as such metabolites were not identified in authentic urine samples. 5FP: 5F-pentyl chain; VA: valine amide; n.d.: not detected in LC-qToF-MS analysis.

\*obtained from LC-qToF-MS analysis only of authentic urine samples.

incubation time, the most abundant OH-metabolite of 5F-AB-P7AICA represented about 5% of the parent compound and the amide hydrolysis only 0.08%. In contrast, the most abundant OH-metabolite showed about 10% of the peak area of 5F-AB-PINACA and the amide hydrolysis product accounted for about 14%. So far, we were not able to identify authentic urine samples with confirmed uptake of 5F-AB-P7AICA (which is usually smoked) to confirm the results after oral administration and we are aware of the possibility that ratios might change in such samples due to the different route of administration or to the different sampling time from intake. Nevertheless, we hypothesize that the 7-AI core is responsible for the reduction of metabolic reactivity.

In a recent paper, Franz et al. demonstrated that the heterocyclic core structure has an impact on several metabolic reactions, and especially on the hydrolysis of terminal or secondary amide functionality. Particularly, indoles were shown to be significantly less reactive than their indazole analogs.<sup>34</sup>

The metabolism of the 7-AI analog of 5F-ADB, 7'-N-5F-ADB, was also recently investigated. The parent compound presented relatively

high peaks in authentic human urine samples, though being the most abundant only in one of four samples.<sup>35</sup> Contrarily, regarding the indazole analog, Yeter et al.<sup>36</sup> showed that in most of the authentic urine samples the concentration of the carboxylic acid metabolite M20 was much higher than the concentration of the parent compound 5F-ADB. This observation supports the hypothesis that the shift of a nitrogen atom from position 2 (indazole) to position 7 (7-AI) significantly lowers the metabolic reactivity.

Overall, the metabolic profile of 5F-AB-P7AICA was very similar to the metabolic profiles of AB-PINACA and 5F-AB-PINACA, the metabolites of which have been studied by means of pHLM and authentic human urine samples.<sup>26,27</sup> Several SCs, such as 5F-MDMB-PICA, AB-FUBINACA and AB-PINACA,<sup>27,37,38</sup> undergo extensive ester/amide hydrolysis. This is one of the main reactions in vivo, although the abundance of ester/amide hydrolysis products, which are mainly produced by carboxylesterases,<sup>39</sup> appeared to be comparatively lower in vitro.<sup>27,38</sup> This effect was particularly seen in the present case, where M13 switched from rank position #12 in pHLM to the rank position #2

in the in vivo sample #07. This is a further confirmation that a verification of pHLM results by analyzing authentic urinary samples, as done in the present work through oral self-administration, is necessary for final selection of reliable marker metabolites.

As described for other 5-fluoropentyl-containing SCs, 5F-AB-P7AICA is subjected to hydrolytic defluorination (M05) and the main fragment ions of the parent compound ( $m/z$  145, 231, 302, 330) are analogous to those found for 5F-AB-PINACA.<sup>27</sup> The metabolic process of hydrolytic defluorination, with the production of a 5-hydroxypentyl-metabolite, is also among the most common for other 5-fluoropentyl analogs. In contrast to the human hepatocytes metabolic profile of 5F-AB-PINACA,<sup>27</sup> in our study no metabolite consistent with a reaction of hydrolytic defluorination and further oxidation to the *N*-pentanoic acid metabolite was shown, neither in vitro nor in vivo by means of LC-qToF-MS analysis for 5F-AB-P7AICA.

In contrast to previously investigated compounds, the parent 5F-AB-P7AICA should be monitored to confirm the uptake of this drug in routine urine screening in addition to the main metabolites, though the ratio among parent compound and metabolites depends on the time of analysis after intake and might change due to smoking consumption. In addition, due to the possibility of different pharmacokinetic patterns in individuals or to a parenteral consumption of the drug, M07 appeared to be a highly specific marker, which could be applied to confirm the intake of 5F-AB-P7AICA by urine analysis and differentiate from other structurally related 7-AI derivatives potentially marketed in the future like 5F-AMB-P7AICA, AB-P7AICA, or AMB-P7AICA. These closely related 7-AI derivatives might in fact share the same carboxylic acid or defluorinated metabolite. The monitoring of M13 is also suggested, since it might be the only detectable substance after a longer time span between 5F-AB-P7AICA intake and sampling.

### 3.4 | Method validation

In the selectivity testing, no interferences with 5F-AB-P7AICA occurred, neither in the blank serum nor in the blank samples containing IS or a mixture of SCs and SC metabolites.

Good linearity was shown for 5F-AB-P7AICA in serum in the concentration range 0.1–30 ng/mL. According to the results of the Mandel test, a linear calibration model was proven, with no need for a weighting factor (correlation coefficients ( $R^2$ ) 0.997).

For the proposed validated method, 0.02 ng/mL and 0.06 ng/mL were defined as the LOD and LOQ, according to Valistat (DIN 32645) using a six-point calibration curve in the range 0.025–0.1 ng/mL.

Accuracy and precision are shown in Table 2, where the results of the matrix effect analysis are also given.

### 3.5 | Preliminary pharmacokinetic data

After validation, the proposed method was successfully applied for the quantification of 5F-AB-P7AICA in serum samples ( $n = 34$ ) collected pre and after a controlled oral self-administration of 2.5 mg of the compound. In Figure 5, the concentration-time profile is displayed.

**TABLE 2** Precision, accuracy bias and matrix effects of the LC-MS/MS method for the quantification of 5F-AB-P7AICA in serum

Substance	Concentration [ng/mL]	Precision [RSD%]	Accuracy [bias %]	Matrix Effect [%]
5F-AB-P7AICA	1	Intra-day (repeatability)	0.8	98
		Inter-day	7.3	
	10	Intra-day (repeatability)	2.2	116
		Inter-day	6.9	

The blank samples collected directly before and after the ingestion tested negative for the compound. 5F-AB-P7AICA was detected and quantified 0.35 hours after the intake, and remained relatively low until 0.85 hours. The compound reached the maximum concentration measured (29.5 ng/mL,  $C_{max}$ ) 2.53 hours ( $T_{max}$ ) after the intake, displaying a relatively rapid gastrointestinal absorption. More than 7 hours later, 10.70 hours after intake, serum concentrations were still above 2.0 ng/mL. The substance remained above the LOQ (0.06 ng/mL) for more than 45 hours and was not detected in the serum sample collected 70.33 hours after the intake.

The comparison of a one-phase and a two-phase pharmacokinetic elimination model allowed to establish that the latter presented a much better fit-to-data, with a probability for the two-phase model of being correct of 97% ( $R^2$  0.9937) according to GraphPad Prism software. The fast phase showed a perceived elimination half-life ( $t_{1/2}$ ) of 0.23 hours and a  $K$  (rate constant) value of 2.96 1/h, while the slow phase had a  $t_{1/2}$  of 2.38 hours and a  $K$  value of 0.29 1/h. During the first plasma decline, the drug that has been absorbed into the central compartment of highly perfused tissues such as kidney, lung and heart, distributes into peripheral/deeper compartments, i.e., less perfused tissues (distribution phase). During the second phase, both re-distribution from the peripheral/deeper compartments and elimination (by metabolism and/or direct excretion) are assumed to occur at the same time. If this is the case, it is likely for the compound to show an accumulation in less perfused tissues such as muscles and fatty tissue after chronic consumption.

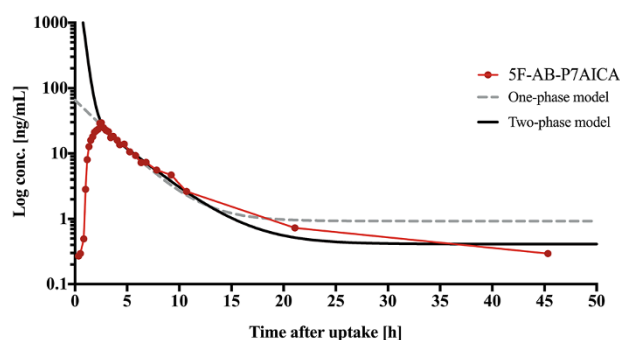


**FIGURE 5** Semi-logarithmic time-concentration profile after a controlled self-administered oral dose of 2.5 mg of 5F-AB-P7AICA and application of a one-phase and a two-phase decay model regression [Colour figure can be viewed at wileyonlinelibrary.com]



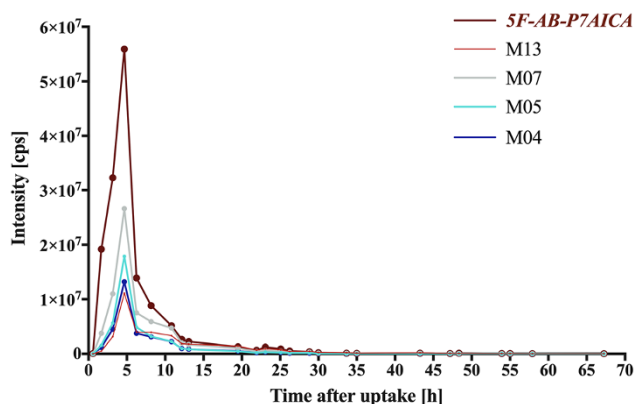


**FIGURE 6** Peak area-time profile, normalized to creatinine concentration, for the parent compound and the four metabolites with the most intense signals after a controlled self-administered oral dose of 2.5 mg of 5F-AB-P7AICA [Colour figure can be viewed at [wileyonlinelibrary.com](http://wileyonlinelibrary.com)]

The volunteer experienced no physical or mental drug-related effects at any stage of the experiment. This was probably due to the low dosage ingested, motivated by the will of limiting potential hazardous effects, the relatively slow resorption after oral ingestion and possibly a first pass effect (extensive first pass effect has been shown for the cannabis constituent THC as well as for other lipophilic compounds).<sup>40,41</sup> However, concentrations reached after oral ingestion were relatively high when compared to those shown for other SCs like AM-2201 under similar conditions.<sup>42</sup> This would again be in line with a relatively low metabolic reactivity of 7-AI core.

None of the main metabolites of 5F-AB-P7AICA, as identified in the *in vitro* and *in vivo* urinary samples, was detected in the serum of the voluntary in its free form (phase II metabolites like glucuronidates were not targeted).

In the authentic urine samples collected after a single controlled oral administration the parent compound, M07 (rank #1), M05 (rank #2), and M13 (rank #4) showed the highest intensities at 4.67 hours post intake, remained above the threshold of MS peak area  $> 1 \times 10^4$  cps for 67 hours (peak areas were normalized for the creatinine levels), and was not detected anymore in a urine sample collected 75.67 hours after the intake. As visible in Figure 6, M07 was the most abundant metabolite in the first 5 hours, showed a plateau from 4.67 hours until 10 hours and then slowly decreased. M05 was in rank position #2 for approximately the first 5 hours, then rapidly decreased, with intensities lower than M13, which, on the contrary, passed from a #4 to a #2 rank position.

The relatively low amount of amide hydrolysis product (M13) when compared to the parent compound and the abundance of the latter could be partially explained by the oral intake of the substance. Since hydrolysis products might be formed during smoking even before entering the body,<sup>43,44</sup> it is reasonable to assume that smoking results in a different ratio of metabolites. However, the amount of hydrolysis products is comparatively low with respect to metabolic hydrolysis.<sup>43,44</sup>

Only a small number of studies investigating human pharmacokinetics of SCs are found in the literature.<sup>45</sup> Thus, data on distribution

and elimination phases widely lacks, especially for new SCs.<sup>45</sup> In the present case, an oral intake was deemed most appropriate in order to avoid severe potential side effects in the absence of data on pharmacodynamics. Indeed, smoking self-experiments retrieved in the literature mostly cover substances which have already been listed as illicit in most of the European countries, and are therefore no longer present on the drug market.<sup>44</sup> A point of strength of the present study is the consideration of a substance with a relatively new core structure (7-AI derivative).

Although these results could be useful for understanding the pharmacokinetics of 5F-AB-P7AICA, a limitation that has to be kept in mind is that SCs are mainly consumed by smoking, and not by oral administration. Parenteral intake could result in stronger effects at the same dose and a differing kinetic profile. Particularly when analyzing urine, higher signal intensities for the amide hydrolysis product could be expected due to artefactual formation of the hydrolysis product during smoking<sup>43,44</sup> or to metabolism in lung, where carboxylesterases are also expressed.<sup>39</sup> However, as previously discussed and confirming data regarding other indole-indazole analogs, it is highly plausible that the shift of a nitrogen atom from position 2 (indazole) to position 7 (7-AI) significantly increases the metabolic stability. A second limitation resides in the fact that data refers to a single volunteer. It is well known that the pharmacokinetic behavior of drugs may vary within different subjects, thus studies on a larger sample are highly encouraged, even though limited by ethical reasons. In the attempt to confirm the *in vivo* results, an *in vitro* comparison between 5F-AB-P7AICA and 5F-AB-PINACA was performed and confirmed the qualitative data. Further, we did not target phase II metabolites in our study because the sample work-up for SCs screening usually involves  $\beta$ -glucuronidase treatment to enhance sensitivity.<sup>38,46</sup>

## 4 | CONCLUSIONS

The present study gives a further example of a wrongly labeled SC sold online as a 'research chemical'. The questionable identity of substances purchased on the Internet could lead to serious adverse events, particularly if drug potencies differ.

The investigated 7-AI analog of 5F-AB-PINACA only partially fit the expected pattern of urinary metabolites, as based on the metabolic profiles of other SCs of the pentyl indole/indazole type and their 5-fluoropentyl analogs. In contrast to previously investigated compounds, the parent 5F-AB-P7AICA should be monitored to confirm the uptake of this drug in routine urine screening in addition to the main metabolites. The hydroxylated metabolite M07 is suggested as a highly specific marker in authentic urine samples with the potential to clearly differentiate from closely related 7-AI derivatives sharing, for example, the same carboxylic acid or defluorinated metabolite. In addition, a validated method to quantify 5F-AB-P7AICA in serum samples was presented, together with preliminary data on pharmacokinetics after oral intake of the drug.

From the presented data, it seems plausible that the shift of the nitrogen atom from position 2 (indazole) to position 7 (7-AI) leads to a lower metabolic reactivity, which might be of interest in terms of the development of medicinal drugs featuring similar structural elements.

## DECLARATION OF INTERESTS

The authors declare no competing financial interests.

## ACKNOWLEDGEMENTS

This publication was funded by the European Union's Justice Programme – Drugs Policy Initiatives (grant agreement number 807055 – NPS-PRISON). The content of this publication represents the views of the authors only and is their sole responsibility. The European Commission does not accept any responsibility for use that may be made of the information it contains. The authors would like to thank the executives of the EU-project ADEBAR (co-funded by the decentral internal security fund, ISF, grant number IZ25-5793-2016-27) for their contribution to our research with the supply of chemical standards. Open access funding enabled and organized by Projekt DEAL. [Correction added on 6 November 2020, after first online publication: Projekt Deal funding statement has been added.]

## ORCID

Arianna Giorgetti  <https://orcid.org/0000-0002-0441-9787>

Lukas Mogler  <https://orcid.org/0000-0001-8987-2785>

Belal Haschimi  <https://orcid.org/0000-0003-2954-7539>

Florian Franz  <https://orcid.org/0000-0001-6158-2882>

Volker Auwärter  <https://orcid.org/0000-0002-1883-2804>

## REFERENCES

- Auwärter V, Dresen S, Weinmann W, Müller M, Pütz M, Ferreirós N. 'Spice' and other herbal blends: harmless incense or cannabinoid designer drugs? *J Mass Spectrom.* 2009;44(5):832-837. <https://doi.org/10.1002/jms.1558>
- Uchiyama N, Kikura-Hanajiri R, Kawahara N, Goda Y. Identification of a cannabimimetic indole as a designer drug in a herbal product. *Forensic Toxicol.* 2009;27(2):61-66.
- European Monitoring Centre for Drugs and Drug Addiction (EMCDDA). European Drug Report; 2019: trends and developments. Publications Office of the European Union, Lisbon. <http://www.emcdda.europa.eu/publications/edr/trends-developments/2019> Accessed July, 17, 2019
- Uchiyama N, Matsuda S, Wakana D, Kikura-Hanajiri R, Goda Y. New cannabimimetic indazole derivatives, N-(1-amino-3-methyl-1-oxobutan-2-yl)-1-pentyl-1H-indazole-3-carboxamide (AB-PINACA) and N-(1-amino-3-methyl-1-oxobutan-2-yl)-1-(4-fluorobenzyl)-1H-indazole-3-carboxamide (AB-FUBINACA) identified as designer drugs in illegal products. *Forensic Toxicol.* 2013;31(1):93-100.
- Uchiyama N, Shimokawa Y, Kawamura M, Kikura-Hanajiri R, Hakamatsuka T. Chemical analysis of a benzofuran derivative, 2-(2-ethylaminopropyl)benzofuran (2-EAPB), eight synthetic cannabinoids, five cathinone derivatives, and five other designer drugs newly detected in illegal products. *Forensic Toxicol.* 2014;32(2):266-281.
- Wiley JL, Marusich JA, Lefever TW, et al. AB-CHMINACA, AB-PINACA, and FUBIMINA: affinity and potency of novel synthetic cannabinoids in producing  $\Delta^9$ -tetrahydrocannabinol-like effects in mice. *J Pharmacol Exp Ther.* 2015;354(3):328-339.
- Banister SD, Moir M, Stuart J, et al. Pharmacology of indole and Indazole synthetic cannabinoid designer drugs AB-FUBINACA, ADB-FUBINACA, AB-PINACA, ADB-PINACA, 5F-AB-PINACA, 5F-ADB-PINACA, ADBICA, and 5F-ADBICA. *ACS Chem Neurosci.* 2015;6(9):1546-1559. <https://doi.org/10.1021/acschemneuro.5b00112>
- WHO Expert Committee on Drug Dependence, thirty-ninth Meeting. AB-PINAC Critical Review Report. Agenda Item 4.4. World Health Organization (WHO Technical Report Series), Geneva. [https://www.who.int/medicines/access/controlled-substances/CriticalReview\\_ABPINACA.pdf?ua=1](https://www.who.int/medicines/access/controlled-substances/CriticalReview_ABPINACA.pdf?ua=1). Accessed August, 21, 2019
- Hutchison RD, Ford BM, Franks LN, et al. Atypical Pharmacodynamic properties and metabolic profile of the abused synthetic cannabinoid AB-PINACA: potential contribution to pronounced adverse effects relative to  $\Delta^9$ -THC. *Front Pharmacol.* 2018;9:1084. <https://doi.org/10.3389/fphar.2018.01084>
- Thornton SL, Akpunonu P, Glauner K, Hoehn KS, Gerona R. Unintentional pediatric exposure to a synthetic cannabinoid (AB-PINACA) resulting in coma and intubation. *Ann Emerg Med.* 2015;66(3):343-344. <https://doi.org/10.1016/j.annemergmed.2015.05.021>
- Armenian P, Darracq M, Gevorkyan J, Clark S, Kaye B, Brandehoff NP. Intoxication from the novel synthetic cannabinoids AB-PINACA and ADB-PINACA: a case series and review of the literature. *Neuropharmacology.* 2018;134:82-91. <https://doi.org/10.1016/j.neuropharm.2017.10.017>
- Yamagishi I, Minakata K, Nozawa H, et al. A case of intoxication with a mixture of synthetic cannabinoids EAM-2201, AB-PINACA and AB-FUBINACA, and a synthetic cathinone  $\alpha$ -PVP. *Leg Med (Tokyo).* 2018; 35:44-49. <https://doi.org/10.1016/j.legalmed.2018.08.004>
- Hasegawa K, Wurita A, Minakata K, et al. Identification and quantitation of 5-fluoro-ADB, one of the most dangerous synthetic cannabinoids, in the stomach contents and solid tissues of a human cadaver and in some herbal products. *Forensic Toxicol.* 2015;33(1): 112-121.
- Kusano M, Zaitu K, Taki K, et al. Fatal intoxication by 5F-ADB and diphenidine: detection, quantification, and investigation of their main metabolic pathways in humans by LC/MS/MS and LC/Q-TOFMS. *Drug Test Anal.* 2018;10(2):284-293. <https://doi.org/10.1002/dta.2215>
- Barceló B, Pichini S, López-Corominas V, et al. Acute intoxication caused by synthetic cannabinoids 5F-ADB and MMB-2201: a case series. *Forensic Sci Int.* 2017;273:e10-e14. <https://doi.org/10.1016/j.forsciint.2017.01.020>
- European Monitoring Centre for Drugs and Drug Addiction (EMCDDA) Report on the risk assessment of methyl 2-[[1-(5-fluoropentyl)-1H-indazole-3-carbonyl]amino]-3,3-dimethylbutanoate (5F-MDMB-PINACA) in the framework of the Council Decision on new psychoactive substances. Publications Office of the European Union, Lisbon. <http://www.emcdda.europa.eu/system/files/publications/9122/Risk%20assessment%205F-MDMB-PINACA.pdf>. Accessed August, 21, 2019
- Immadi SS, Dopart R, Wu Z, Fu B, Kendall DA, Lu D. Exploring 6-Azaindole and 7-Azaindole rings for developing cannabinoid receptor 1 allosteric modulators. *Cannabis Cannabinoid Res.* 2018;3(1):252-258. <https://doi.org/10.1089/can.2018.0046>
- Banister SD, Adams A, Kevin RC, et al. Synthesis and pharmacology of new psychoactive substance 5F-CUMYL-P7AICA, a scaffold-hopping analog of synthetic cannabinoid receptor agonists 5F-CUMYL-PICA and 5F-CUMYL-PINACA. *Drug Test Anal.* 2019;11(2):279-291. <https://doi.org/10.1002/dta.2491>
- Sobolevsky T, Prasolov I, Rodchenkov G. Detection of JWH-018 metabolites in smoking mixture post-administration urine. *Forensic*

- science international, 200, 141–147. *Forensic Sci Int.* 2010;200(1–3): 141–147. <https://doi.org/10.1016/j.forsciint.2010.04.003>
20. Sobolevsky T, Prasolov I, Rodchenkov G. Detection of urinary metabolites of AM-2201 and UR-144, two novel synthetic cannabinoids. *Drug testing and analysis*, 4, 745–753. *Drug Test Anal.* 2012;4(10): 745–753. <https://doi.org/10.1002/dta.1418>
  21. Diao X, Huestis MA. New synthetic cannabinoids metabolism and strategies to best identify optimal marker metabolites. *Front Chem.* 2019;7(109):1–15.
  22. Knittel JL, Holler JM, Chmiel JD, et al. Analysis of parent synthetic cannabinoids in blood and urinary metabolites by liquid chromatography tandem mass spectrometry. *J Anal Toxicol.* 2016;40(3):173–186. <https://doi.org/10.1093/jat/bkv137>
  23. Moosmann B, Kneisel S, Girreser U, Brecht V, Westphal F, Auwärter V. Separation and structural characterization of the synthetic cannabinoids JWH-412 and 1-[(5-fluoropentyl)-1H-indol-3-yl]-4-methylnaphthalen-1-yl)methanone using GC–MS, NMR analysis and a flash chromatography system. *Forensic Sci Int.* 2012;220(1): e17–e22.
  24. Mogler L, Franz F, Wilde M, et al. Phase I metabolism of the carbazole-derived synthetic cannabinoids EG-018, EG-2201, and MDMB-CHMCA and detection in human urine samples. *Drug Test Anal.* 2018;10(9):1417–1429. <https://doi.org/10.1002/dta.2398>
  25. Mogler L, Halter S, Wilde M, Franz F, Auwärter V. Human phase I metabolism of the novel synthetic cannabinoid 5F-CUMYL-PEGACLONE. *Forensic Toxicol.* 2019;37(1):154–163. <https://doi.org/10.1007/s11419-018-0447-4>
  26. Takayama T, Suzuki M, Todoroki K, et al. UPLC/ESI-MS/MS-based determination of metabolism of several new illicit drugs, ADB-FUBINACA, AB-FUBINACA, AB-PINACA, QUPIC, 5F-QUPIC and  $\alpha$ -PVT, by human liver microsome. *Biomed Chromatogr.* 2014;28(6): 831–838. <https://doi.org/10.1002/bmc.3155>
  27. Wohlfarth A, Castaneto MS, Zhu M, et al. Pentylindole/Pentylindazole synthetic cannabinoids and their 5-fluoro analogs produce different primary metabolites: metabolite profiling for AB-PINACA and 5F-AB-PINACA. *AAPS J.* 2015;17(3): 660–677.
  28. Peters FT, Drummer OH, Musshoff F. Validation of new methods. *Forensic Sci Int.* 2007;165(2–3):216–224.
  29. German Society of Toxicological and Forensic Chemistry (GTFCh) Guidelines for quality assurance in forensic-toxicological analyses. <https://www.gtfch.org/cms/images/stories/files/Appendix%20B%20GTFCh%2020090601.pdf>. Accessed July, 17, 2019
  30. Matuszewski BK, Constanzer ML, Chavez-Eng CM. Strategies for the assessment of matrix effect in quantitative bioanalytical methods based on HPLC-MS/MS. *Anal Chem.* 2003;75(13):3019–3030.
  31. NPS Data-Hub. <https://www.nps-datahub.com>. Accessed August, 19 2019
  32. ADEBAR Project. 5F-AB-P7AICA Analytical Report [https://www.policija.si/apps/nfl\\_response\\_web/0\\_Analytical\\_Reports\\_final/5F-AB-P7AICA-ID-ADB-18\\_076\\_report.pdf](https://www.policija.si/apps/nfl_response_web/0_Analytical_Reports_final/5F-AB-P7AICA-ID-ADB-18_076_report.pdf). Accessed August, 19 2019
  33. Shevyrin V, Melkozherov V, Nevero A, et al. Identification and analytical characteristics of synthetic cannabinoids with an indazole-3-carboxamide structure bearing a N-1-methoxycarbonylalkyl group. *Anal Bioanal Chem.* 2015;407(21):6301–6315. <https://doi.org/10.1007/s00216-015-8612-7>
  34. Franz F, Jechle H, Wilde M, et al. Structure-metabolism relationships of valine and tert-leucine-derived synthetic cannabinoid receptor agonists: a systematic comparison of the in vitro phase I metabolism using pooled human liver microsomes and high-resolution mass spectrometry. *Forensic Toxicol.* 2019;37(2):316–329. <https://doi.org/10.1007/s11419-018-00462-x>
  35. Richter LHJ, Maurer HH, Meyer MR. Metabolic fate of the new synthetic cannabinoid 7N-5F-ADB in rat, human, and pooled human S9 studied by means of hyphenated high-resolution mass spectrometry. *Drug Test Anal.* 2019;11(2):305–317. <https://doi.org/10.1002/dta.2493>
  36. Yeter O, Ozturk YE. Metabolic profiling of synthetic cannabinoid 5F-ADB by human liver microsome incubations and urine samples using high-resolution mass spectrometry. *Drug Test Anal.* 2019;11(6): 847–858. <https://doi.org/10.1002/dta.2566>
  37. Castaneto MS, Wohlfarth A, Pang S, et al. Identification of AB-FUBINACA metabolites in human hepatocytes and urine using high-resolution mass spectrometry. *Forensic Toxicol.* 2015;33(2):295–310. <https://doi.org/10.1007/s11419-015-0275-8>
  38. Mogler L, Franz F, Rentsch D, et al. Detection of the recently emerged synthetic cannabinoid 5F-MDMB-PICA in 'legal high' products and human urine samples. *Drug Test Anal.* 2018;10(1):196–205. <https://doi.org/10.1002/dta.2201>
  39. Thomsen R, Nielsen LM, Holm NB, Rasmussen HB, Linnet K. INDICES consortium. Synthetic cannabimimetic agents metabolized by carboxylesterases. *Drug Test Anal.* 2015;7(7):565–576. <https://doi.org/10.1002/dta.1731>
  40. Ohlsson A, Lindgren JE, Wahlen A, Agurell S, Hollister LE, Gillespie HK. Plasma delta-9 tetrahydrocannabinol concentrations and clinical effects after oral and intravenous administration and smoking. *Clin Pharmacol Ther.* 1980;28(3):409–416.
  41. Huestis MA. Human cannabinoid pharmacokinetics. *Chem Biodivers.* 2007;4(8):1770–1804. <https://doi.org/10.1002/cbdv.200790152>
  42. Hutter M, Moosmann B, Kneisel S, Auwärter V. Characteristics of the designer drug and synthetic cannabinoid receptor agonist AM-2201 regarding its chemistry and metabolism. *J Mass Spectrom.* 2013;48(7): 885–894. <https://doi.org/10.1002/jms.3229>
  43. Franz F, Angerer V, Moosmann B, Auwärter V. Phase I metabolism of the highly potent synthetic cannabinoid MDMB-CHMICA and detection in human urine samples. *Drug Test Anal.* 2017;9(5):744–753. <https://doi.org/10.1002/dta.2049>
  44. Franz F, Angerer V, Hermanns-Clausen M, Auwärter V, Moosmann B. Metabolites of synthetic cannabinoids in hair—proof of consumption or false friends for interpretation? *Anal Bioanal Chem.* 2016;408(13): 3445–34452. <https://doi.org/10.1007/s00216-016-9422-2>
  45. Castaneto MS, Wohlfarth A, Desrosiers NA, Hartman RL, Gorelick DA, Huestis MA. Synthetic cannabinoids pharmacokinetics and detection methods in biological matrices. *Drug Metab Rev.* 2015; 47(2):124–174. <https://doi.org/10.3109/03602532.2015.1029635>
  46. Carlier J, Diao X, Scheidweiler KB, Huestis MA. Distinguishing intake of new synthetic cannabinoids ADB-PINACA and 5F-ADB-PINACA with human hepatocyte metabolites and high-resolution mass spectrometry. *Clin Chem.* 2017;63(5):1008–1021. <https://doi.org/10.1373/clinchem.2016.267575>

## SUPPORTING INFORMATION

Additional supporting information may be found online in the Supporting Information section at the end of this article.

**How to cite this article:** Giorgetti A, Mogler L, Haschimi B, et al. Detection and phase I metabolism of the 7-azaindole-derived synthetic cannabinoid 5F-AB-P7AICA including a preliminary pharmacokinetic evaluation. *Drug Test Anal.* 2020;12: 78–91. <https://doi.org/10.1002/dta.2692>